^{7}Li and ^{51}V NMR study of the heavy-fermion compound LiV_2O_4

A. V. Mahajan,* R. Sala,† E. Lee, F. Borsa,† S. Kondo, and D. C. Johnston
Ames Laboratory and Department of Physics and Astronomy, Iowa State University, Ames, Iowa 50011
(Received 30 October 1997)

^{7}Li and ^{51}V NMR Knight shift, linewidth, spin-lattice, and spin-spin relaxation rate data are reported as a function of temperature T (1.5–800 K and 74–575 K for Li and V nuclei, respectively) in the heavy fermion compound LiV_2O_4. The ^{7}Li Knight shift K exhibits a broad maximum at about 25 K and is nearly constant below 4.2 K, as is the linewidth. The ^{51}V Knight shift is negative at 575 K and it decreases strongly as the temperature is lowered. Above ~80 K, both ^{7}Li and ^{51}V Knight shifts are proportional to the susceptibility and from the slope the hyperfine coupling constant can be obtained for both nuclei. The ^{7}Li spin-lattice relaxation rate increases as the temperature is lowered below room temperature reaching a maximum at about 50 K. Below 5 K the relaxation rate decreases linearly with T as for normal metals but with a very high value of the Korringa product $(T_1T)^{-1}$. Even so, the ^{7}Li Korringa ratio K^2T_1T/S_{Li} below ~ 10 K is on the order of unity as in conventional metals, thus indicating heavy Fermi liquid behavior. From an analysis of the ^{7}Li and ^{51}V relaxation rate data we infer an approximate square root temperature dependence of the V local moment spin-relaxation rate at high temperatures ($T \gtrsim 50$ K). A simplified analysis of the data yields a value of 17 meV for the magnitude of the exchange coupling constant between the local moments and the conduction electrons and 2.3 meV for that between neighboring local moments. Quantitative discrepancies in the ^{7}Li and ^{51}V relaxation rates at low T from what is expected for a uniform heavy Fermi liquid indicate that effects such as Kondo effect screening of the V local moment and/or dynamical vanadium t_{2g} orbital occupation correlation/fluctuation effects may be present in our system. [S0163-1829(98)00715-2]

I. INTRODUCTION

There is currently great interest in understanding the behavior of strongly correlated metallic systems. While there is adequate theoretical understanding of systems in the free-electron limit or in the case of localized moments, systems that have competing electron correlation and transfer effects can show unusual properties and are theoretically difficult to describe. Metals doped with dilute amounts of magnetic impurities have been investigated in the past to understand any modifications of the magnetic properties of the doped impurity as well as the host atoms. The Kondo effect, which involves a quenching of the impurity local moment, was discovered then. On the other hand, metallic systems involving a high concentration of local moments also exhibit interesting physical phenomena. In particular, systems such as some RAl_3 (R denotes rare earth) compounds, $CeCu_2Si_2$, etc.[1] show a crossover to heavy-fermion behavior at low temperatures, wherein the $4f$ local moments are quenched and the carriers are inferred to have very high effective masses ($\gtrsim 100m_e$, where m_e is the electron mass).

Nuclear magnetic resonance (NMR) has, in the past, provided valuable information regarding fundamental issues such as formation of local moments in metals in the dilute limit, Kondo effect, magnetic fluctuations and ordering, heavy-fermion behavior, etc. via a study of the magnitude and the temperature T variation of the Knight shift K, linewidth Δ, and the spin-spin $(1/T_2)$ and the spin-lattice $(1/T_1)$ relaxation rates.

More recently, NMR in the cuprate high-T_c compounds has helped in understanding the strongly correlated electronic state. We have been involved in investigating compounds analogous to the Cu-based materials. Vanadium-based oxides that have a mixture of V^{3+} $(3d^2)$ and V^{4+} $(3d^1)$ are particularly interesting since they can be thought of as electron analogs of the cuprates that have 1–2 holes per Cu. LiV_2O_4 has the cubic spinel structure with the vanadium atoms occupying octahedral sites and the Li atoms occupying tetrahedral sites.[2] Since the formal oxidation state of V is nonintegral (+3.5) and the V ions are crystallographically equivalent, LiV_2O_4 must be metallic as is observed.[3] Heavy-fermion behavior in LiV_2O_4 has recently been discovered.[4] At high T, the magnetic susceptibility $\chi(T)$ can be fit by the sum of a T-independent term χ_0 and a Curie-Weiss $[C/(T-\theta)]$ spin term with an effective moment close to that expected from a spin $S=1/2$ ion and a Weiss temperature θ in the range of -12 to -60 K, depending on the T range of the fit below ~400 K.[5] This suggests that one electron is localized on the V ion and the V local moments have antiferromagnetic interactions between them.

Until the work of Ref. 4, and independently Ref. 6, $\chi(T)$ measurements on LiV_2O_4 have found an increasing susceptibility with decreasing T (down to 4 K). ^{7}Li and ^{51}V NMR measurements on these samples detected a shift that scaled with the susceptibility, an increasing relaxation rate with decreasing T, and a Curie-Weiss-like linewidth.[7,8] The ^{7}Li NMR measurements that we report here pertain to new high-quality samples for which the susceptibility starts deviating from the Curie-Weiss law around 50–100 K and exhibits a broad weak maximum around 16 K (see Fig. 1). With a combination of bulk susceptibility, heat capacity, muon spin relaxation (μSR), and NMR on these relatively defect free and pure samples we and collaborators have established[4] that LiV_2O_4 exhibits a crossover from a combination of local

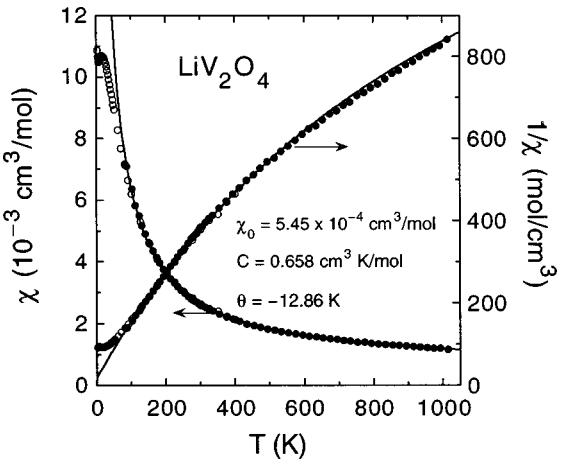

FIG. 1. Magnetic susceptibility $\chi \equiv M/H$ ($H = 10$ kG) vs T in LiV_2O_4 from our present work [(○), sample 3-3-q1] and Ref. 21 (●). The solid lines are the best fit curves according to Eq. (4).

moments and itinerant electrons at high T to a heavy Fermi liquid at low T. In the following we present a detailed analysis of our ^{7}Li and ^{51}V NMR measurements in LiV_2O_4.

II. EXPERIMENTAL DETAILS

The data reported here pertain to samples on which resistivity, susceptibility, heat capacity, x-ray and/or neutron diffraction, and/or μSR measurements (reported in Refs. 4 and 5) were carried out. The details regarding sample preparation can be found in Ref. 5.

^{7}Li and ^{51}V NMR measurements have been performed with a phase-coherent pulse spectrometer.[9] K, Δ, T_1, and T_2 of ^{7}Li were measured in the T range 1.5 to 800 K in applied fields of 1, 1.5, 2 (electromagnet), 4.7, and 8.2 T (superconducting magnets). K, Δ, and T_1 of ^{51}V were measured from 74 to 575 K in an applied field of 4.7 T; a few measurements were done at low field (1.5 T) and low temperature (4.2–1.5 K). The shift was measured with respect to an aqueous LiCl and an aqueous $AlCl_3$ solution for ^{7}Li and ^{51}V, respectively. The ^{7}Li T_1 was determined by monitoring the recovery of nuclear magnetization following a $\pi/2$ pulse (pulse width = 3 μsec) and the ^{51}V T_1 has been determined from the recovery of the spin echo intensity following a saturation sequence of 5–10 $\pi/2$ pulses (pulse width = 4 μsec). T_2 was determined from the variation of the echo height with delay between two $\pi/2$ reading pulses. The linewidth has been measured by taking the full width at half maximum (FWHM) intensity of the Fourier transform of the free induction decay (^{7}Li) and of the spin echo signal (^{51}V). A pumped ^{4}He cryostat was used for temperatures between 1.5 and 4.2 K. For measurements between 4.2 and 300 K, the temperature was varied with an Oxford continuous flow cryostat. To attain temperatures above 300 K we used a furnace with nitrogen exchange gas.

III. RESULTS

A. ^{7}Li NMR

Since the Li nucleus (nuclear spin $I = 3/2$) is at a site of cubic symmetry, we observe a single NMR line without quadrupolar effects. The ^{7}Li shift K is then reliably obtained from the peak position. The variation of K with T is shown in Fig. 2; an expanded plot of the data below 100 K is shown in the inset. We see that the shift increases in a Curie-Weiss-like manner with decreasing T and has a broad peak around 25–30 K, in accord with bulk susceptibility data[4] (see Fig. 1). The Curie-Weiss-like increase of the shift with decreasing T is indicative of local (or quasilocal) moments at the vanadium sites in the sample.

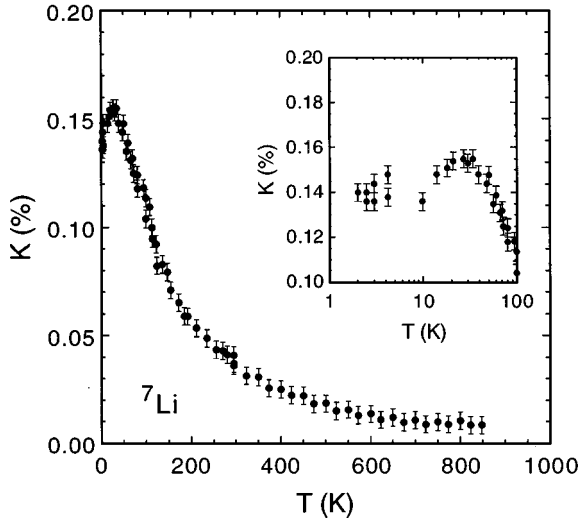

FIG. 2. ^{7}Li Knight shift K vs temperature T in LiV_2O_4. An expanded plot of the data below 100 K is shown in the inset. Samples 3-3, 3-3-q1, 4-0-1, and 12-1 yield nearly identical results.

From Fig. 3 K is seen to vary approximately linearly with the local moment susceptibility above 100 K [see Eq. (3) below], with T as an implicit parameter. The slope yields the hyperfine coupling constant and is further analyzed in Sec. IV A. The deviation from linearity at low T seen here has also been seen in, e.g., $CeAl_3$ (^{27}Al NMR), a heavy fermion compound.[10] Such nonlinearity is expected, on theoretical grounds, for heavy fermion compounds at low T.[11]

In samples with relatively higher impurity Curie terms in the susceptibility we find that at low T ($\approx$20 K), the ^{7}Li NMR line shape becomes asymmetric with apparently a sec-

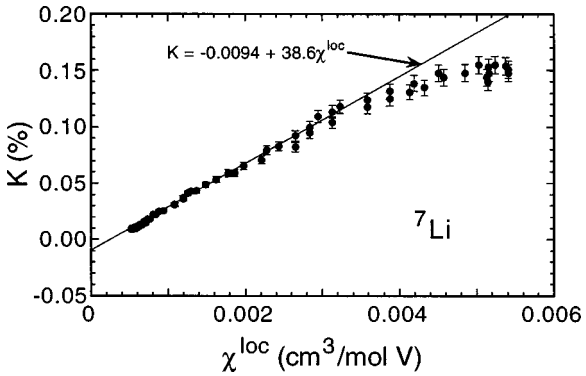

FIG. 3. ^{7}Li Knight shift K vs the local moment susceptibility χ^{loc} per mole V [see Eqs. (2)–(4) in the text] in sample 12-1. The χ^{loc} is the one obtained from the best fit according to Eq. (4) in the text for the susceptibility data in Fig. 1. The line is a linear fit to the data above 100 K.

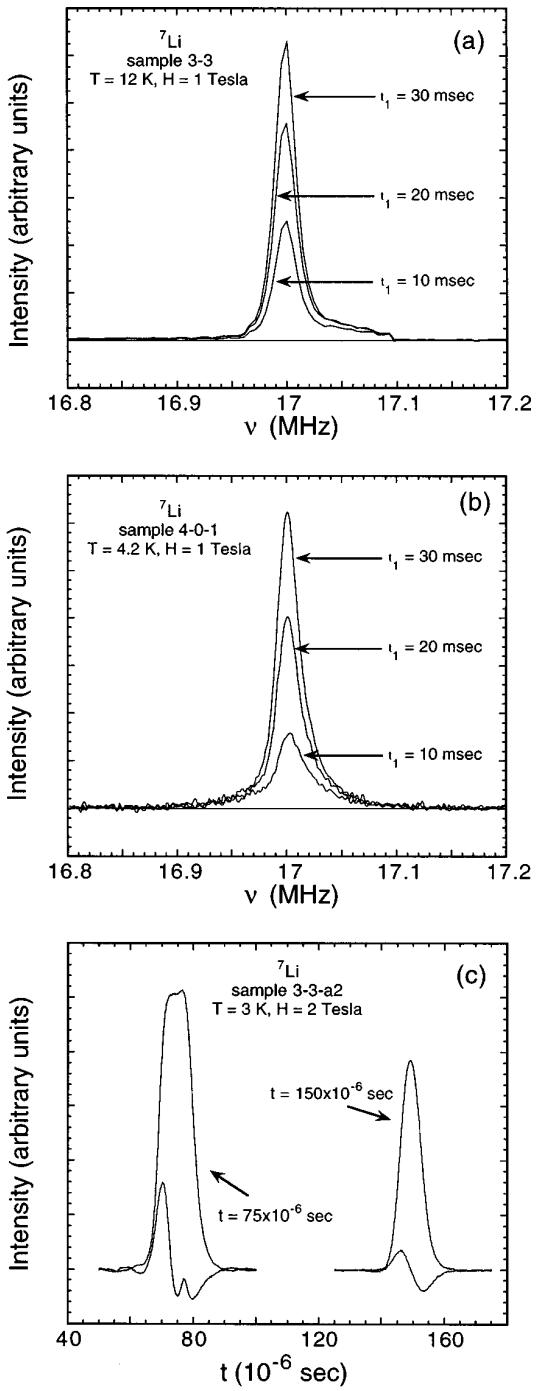

FIG. 4. (a) ^{7}Li NMR line shape (for sample 3-3) as obtained from the Fourier transform of the echo signal following the pulse sequence $\pi/2$- t_1-($\pi/2$-t_2-$\pi/2$) with $t_2 = 150\times10^{-6}$ sec and t_1 varying as indicated in the figure. (b) Same as above, but for sample 4-0-1, which has lower amounts of paramagnetic (Curie term) impurities, as inferred from bulk magnetization measurements. (c) ^{7}Li NMR echo shape in sample 3-3-a2 (which has higher amounts of paramagnetic impurities) following a pulse sequence $\pi/2$-t-$\pi/2$ for two time delays t as indicated in the figure. The horizontal scale is the time elapsed following the second $\pi/2$ pulse.

ond broad line on the high-shift side [Fig. 4(a)] with an intensity of a few percent of the total intensity. Using short (compared to T_1 of the main line) delays between the saturating and the probing pulse it is seen that the second line is enhanced relative to the main line. This indicates that the second line has a shorter T_1. This could be due to a small fraction of the vanadium atoms occupying the tetrahedral sites that are crystallographically and magnetically inequivalent to the octahedral sites. A moment localized at these sites could give rise to the second line through an indirect hyperfine coupling via the conduction electrons to the near-neighbor ^{7}Li nuclei. This broad, fast relaxing feature is less prominent in samples with smaller Curie terms in the susceptibility [see Fig. 4(b) and Table I]. This is presumably related to a smaller fraction of magnetic defect species in these samples. In addition, at lower temperatures (<10–15 K) the shape of the spin echo seems to imply the presence of an additional signal with a phase different from the main signal [see Fig. 4(c)]. For longer delays between the two $\pi/2$ pulses this additional feature disappears, indicating that it has a shorter T_2. The shorter T_2 might be due to local moments in the vicinity of the Li nuclei and the peculiar shape of the echo signal might indicate the presence of some structural distortions (at a local level) at low temperatures, lowering the symmetry of some of the Li sites. Quadrupolar effects become relevant due to this and the smaller $\pi/2$ pulse width observed might be expected if only the central line is irradiated. In a defect free and perfectly ordered sample, these effects would presumably be absent. We note that x-ray[4] and neutron[4,12] diffraction measurements on these samples found no evidence for a structural phase transition from 295 down to 4 K.

The ^{7}Li NMR linewidth Δ was found to be field dependent, indicating that the broadening is inhomogeneous. Δ increases with decreasing T, as shown in Fig. 5, in a way approximately proportional to the magnetic susceptibility. We found that the width depends on the sample preparation procedure, the linewidth being lowest in the ''best'' [having a clear plateau and/or peak in $\chi(T\simeq 20$ K) and having low amounts of extrinsic paramagnetic Curie-term impurities] samples (see Table I). Finally, Δ seems to level off below about 30 K, in qualitative agreement with the susceptibility. Our experimental data are in good agreement with previous results,[13,14] which were obtained mostly at low fields. The authors of Ref. 14 analyze the ^{7}Li NMR linewidth in terms of a contribution from dipole-dipole interaction and a contribution from the distribution of local fields due to demagnetization effects. In the following we perform the same analysis to explain the ^{51}V NMR linewidth data. The conclusion is that for both ^{7}Li and ^{51}V the linewidth is dominated at low T and high field by macroscopic magnetization effects and thus it does not provide useful information besides that already obtained from the susceptibility.

The ^{7}Li nuclear spin-lattice relaxation rate $1/T_1$ was determined by fitting the nuclear magnetization recovery, following a $\pi/2$ pulse, to an exponential. The recovery was found to be a single exponential over the entire temperature range (1.5–800 K). The T variation of ^{7}Li $1/T_1$ is shown in Fig. 6. $1/T_1$ first increases linearly with T, goes through a maximum at about 50 K, and then decreases at higher temperatures. We note here that in the case of metallic $LiTi_2O_4$, which is isostructural to LiV_2O_4, the ^{7}Li NMR spin-lattice relaxation rate follows a Korringa law[15] ($1/T_1 \propto T$) between 20 and 300 K,[16] in strong contrast to our data in LiV_2O_4. At room temperature the ^{7}Li $1/T_1$ in LiV_2O_4 is about 100 times

TABLE I. Summary of the ''impurity'' concentration n deduced from analyses of low-I magnetization data (Refs. 4 and 5). Also shown are the Korringa products $(T_1T)^{-1}$ and the Korringa ratios K^2T_1T/S_{Li} obtained from the ^{7}Li NMR data in the low-T range (1.5−4.2 K) [see Figs. 2 and 6(b)].

Sample designation (Present work)	Sample designation (in Ref. 4)	n (mol %)	$(T_1T)^{-1}$ ($\mathrm{sec}^{-1}\,\mathrm{K}^{-1}$)	K^2T_1T/S_{Li}
4-0-1	1	0.03	2.25±0.05	0.55±0.1
3-3	2	0.35	2.5±0.1	0.50±0.1
3-3-q1	4	0.08	2.20±0.05	0.57±0.1
12-1		0.02	2.25±0.05	0.55±0.1
3-3-a2		1.2	3.0±0.1	0.42±0.1

that in $LiTi_2O_4$. Below about 10 K (in LiV_2O_4), where K is nearly constant, $1/T_1$ varies linearly with T, implying the validity of a Fermi-liquid picture (the minimum $1/T_1T=2.25$ $\mathrm{sec}^{-1}\,\mathrm{K}^{-1}$ for various samples, as opposed to a value of 5.6×10^{-4} $\mathrm{sec}^{-1}\,\mathrm{K}^{-1}$ in $LiTi_2O_4$). Even for samples in which the bulk susceptibility does not show a clear peak around 20 K due to the presence of paramagnetic defects and/or impurities the relaxation rate is Korringa-like below 4 K. This indicates that the Fermi-liquid state is robust and insensitive to small changes in stoichiometry, defect-level and/or site occupation. The low-T behavior for various samples is shown in Fig. 6(b) and Table I. Figure 7 shows the T variation of K^2T_1T scaled by $S=1.74\times10^{-6}$ sec K, the value expected for a ^{7}Li nucleus in a free electron picture.[15] K^2T_1T/S shows an increase with a decrease in T below 800 K, has a maximum around 100 K, and decreases at lower T. Interestingly, these variations are qualitatively similar to those observed in ^{27}Al NMR of the heavy-fermion compound $CeAl_3$.[10] The spin-spin relaxation rate $1/T_2$ shown below 260 K in Fig. 8 is nearly T independent, suggesting that it is dominated by nuclear dipole-dipole interactions.

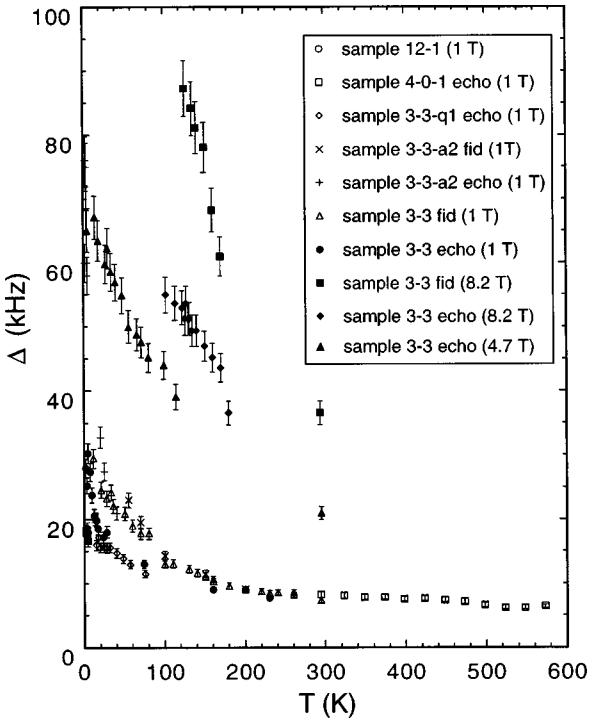

FIG. 5. Variation of the ^{7}Li NMR linewidth Δ (full width at half maximum) with temperature T for various LiV_2O_4 samples. The linewidth is larger at higher fields and the linewidth determined from the Fourier transform (FT) of the free induction decay is larger than that determined from the FT of the echo.

B. ^{51}V NMR

The structure[2] of LiV_2O_4 contains crystallographically equivalent V ions (nuclear spin $I=7/2$) in slightly distorted octahedral coordination with O; thus quadrupole effects are possible. Because we found the $\pi/2$ pulse length on the ^{51}V nuclei to be the same as the $\pi/2$ pulse length on the ^{27}Al nuclei in a reference solution with identical coil and power conditions (^{51}V and ^{27}Al have almost the same γ), we can

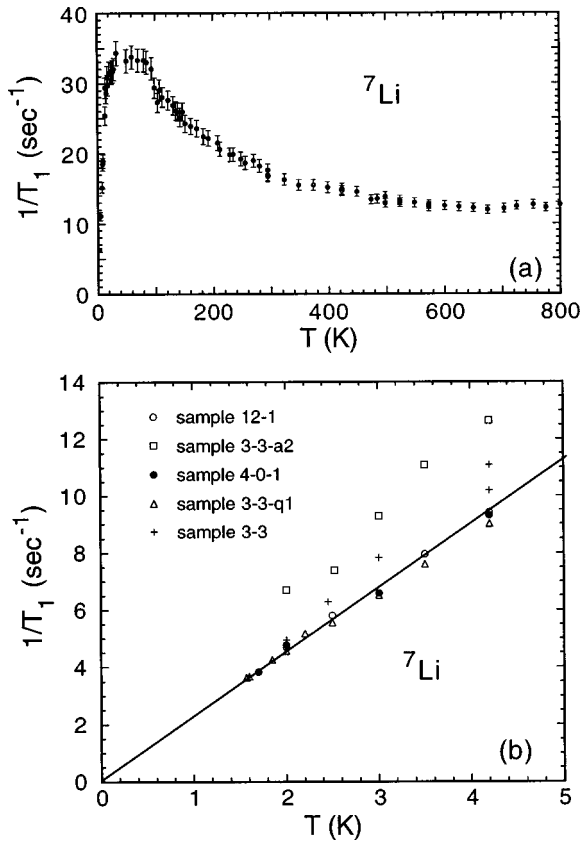

FIG. 6. (a) ^{7}Li nuclear spin-lattice relaxation rate $1/T_1$ vs temperature T for sample 3-3. (b) ^{7}Li nuclear spin-lattice relaxation rate vs temperature ($T<4.2$ K) for samples 3-3, 3-3-a2, 3-3-q1, 4-0-1, and 12-1. The straight line corresponds to the Korringa product $(T_1T)^{-1}=2.25$ $\mathrm{sec}^{-1}\,\mathrm{K}^{-1}$.

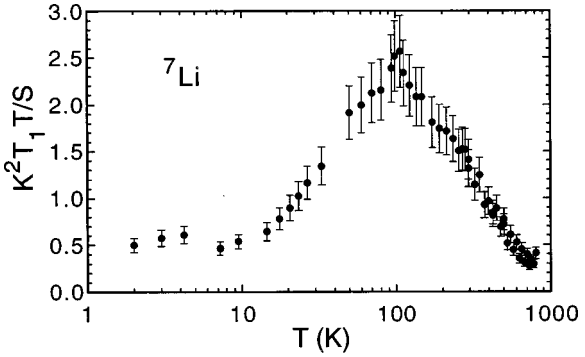

FIG. 7. The Korringa ratio K^2T_1T/S vs temperature T from ^{7}Li NMR for LiV_2O_4 (sample 3-3).

conclude that both the central transition line ($+\frac{1}{2}\leftrightarrow-\frac{1}{2}$) and the satellite lines ($\pm\frac{1}{2}\leftrightarrow\pm\frac{3}{2}\leftrightarrow\pm\frac{5}{2}\leftrightarrow\pm\frac{7}{2}$) are irradiated by the RF pulse. Quadrupole effects are thus negligible. The ^{51}V linewidth was found to be both temperature and field dependent, as shown in Fig. 9. The formal oxidation state is $V^{+3.5}$. The presence of only one ^{51}V line rules out the possibility of having different moments on the V^{3+} and V^{4+} with a lifetime longer than the time window of the NMR experiment, i.e., 10^{-6} sec. The ^{51}V linewidth can be interpreted in terms of a T- and an H-independent contribution from the nuclear ^{51}V-^{51}V and ^{51}V-^{7}Li dipolar interaction[17] and a T- and an H-dependent contribution from macroscopic field inhomogeneities due to the demagnetization effects of a powder sample.[18] By using a Gaussian approximation we can write for the ^{51}V linewidth

$$\Delta_{\mathrm{FWHM}}=2.35\sqrt{\langle\Delta\nu^2\rangle_{\mathrm{dip}}+(B\chi_V H\gamma/2\pi)^2}, \qquad (1)$$

where χ_V is the measured volume susceptibility ($\chi_V=\chi_M d/M$, $d=4.105$ g/cm^3 is the density, and $M=173$ g/mol is the molar mass), $\gamma/2\pi=1119.3$ Hz G^{-1} and B is the fractional root-mean-square deviation of the local field from the applied field H. Using the lattice constant $a=8.24$ Å, the contribution to the second moment obtained from the Van Vleck[17] formula is $\langle\Delta\nu^2\rangle_{\mathrm{dip}}=\langle\Delta\nu^2\rangle_{\mathrm{V\text{-}V}}+\langle\Delta\nu^2\rangle_{\mathrm{V\text{-}Li}}=4.6\times10^7$ Hz$^2+0.41\times10^7$ Hz$^2=5.0\times10^7$ Hz^2. A fit of the measured linewidth using Eq. (1) with B the only fitting parameter yields the solid curve in the inset of Fig. 9 with $B=3.6$. The value of B estimated for a powder of closely

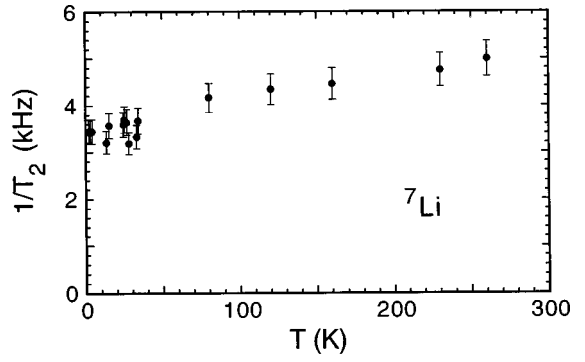

FIG. 8. The ^{7}Li nuclear spin-spin relaxation rate $1/T_2$ vs temperature T in LiV_2O_4 (sample 3-3).

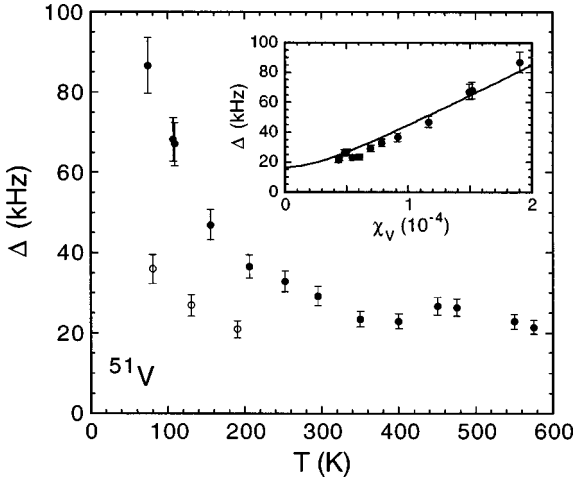

FIG. 9. ^{51}V NMR linewidth Δ (full width at half maximum), obtained from the FT of the echo signal in a magnetic field of 1.5 T (○) and 4.7 T (●) (sample 12-1), vs temperature T. In the inset the same data are plotted as a function of the local moment volume susceptibility χ_V; the solid curve represents Eq. (1) in the text, with $B=3.6$.

packed spheroids[18] is $B=4\pi\times0.114=1.43$. An additional contribution to the local magnetic field distribution can arise from the dipolar sum inside the Lorentz cavity since the ^{51}V nucleus is located at a point of noncubic symmetry with respect to the surrounding V local moments. Thus the ^{51}V linewidth can be explained entirely by assuming that all the V local moments carry the same average moment. As mentioned before a similar analysis can be used to explain the ^{7}Li linewidth in Fig. 5. The details of the analysis will not be repeated here since they are the same as in Ref. 14. We conclude that both the ^{51}V and the ^{7}Li linewidth can be explained without the need to assume different local moments at the V sites.

The ^{51}V Knight shift K versus temperature is reported in Fig. 10. It is negative, strongly temperature dependent, and directly proportional to the susceptibility above 74 K (see inset in Fig. 10).

The ^{51}V nuclear spin lattice relaxation rate has been de-

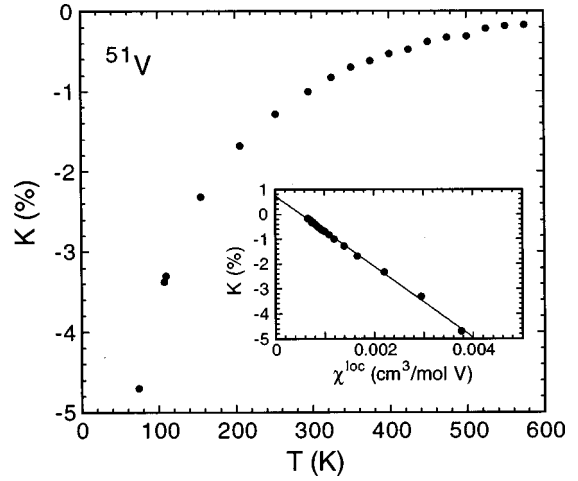

FIG. 10. ^{51}V Knight shift K vs temperature T and, in the inset, vs the local moment susceptibility χ^{loc} (sample 12-1). The solid straight line in the inset is a linear fit to the data (see text).

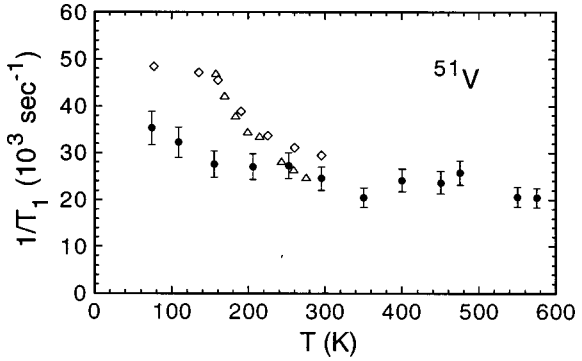

FIG. 11. ^{51}V nuclear spin-lattice relaxation rate $1/T_1$ vs temperature T; our data [(●), sample 12-1] are compared with data from Ref. 14 (◇) and from Ref. 13 (△).

termined from the recovery of the echo amplitude following a saturation comb. The recovery is found to be exponential over the entire temperature range investigated, 74 to 575 K. In Fig. 11 we report our $1/T_1$ data and compare them with data from the literature.[13,14] The signal is lost below 74 K because T_2 becomes very short. It is noted that the big error bars on our relaxation data in Fig. 11 are due to the fact that T_1 is very short and is comparable to T_2, thus making it difficult to obtain the initial condition of complete saturation or of inversion of the magnetization. At room temperature our data are in agreement with the previous ones.[13,14] The disagreement found at lower temperatures is not presently understood. A search for the ^{51}V NMR signal with our spectrometer in the temperature range 1.5–4.2 K was unsuccessful. Since the ^{51}V signal has been observed at low T by continuous wave techniques at low fields[14] ($H<1.5$ T), we are led to the conclusion that the ^{51}V T_1 and/or T_2 must be so short at low T that the free induction decay falls entirely inside the dead time of the receiver ($T_{1,2}\leqslant 5$ μsec).

IV. ANALYSIS AND DISCUSSION

A. High-temperature ^{7}Li and ^{51}V NMR results

1. Knight shift

We now discuss the high-T ($\gtrsim$50 K) ^{7}Li data in the context of a V local moment picture. The ^{7}Li nuclei can be coupled via a direct dipolar coupling to the V local moment and via exchange hyperfine coupling to the V moment and conduction electrons, both of which have d character. In addition, one can have a partial s character to the electrons at the Fermi level, which will give rise to a shift of the ^{7}Li NMR line via the usual Fermi contact interaction. Since the trace of the dipolar coupling tensor is zero, a shift caused by the dipolar coupling (in our polycrystalline samples) will arise only in the presence of a g-factor anisotropy. In the expression for the NMR lineshift due to the dipolar and hyperfine interactions with local moments (in the presence of an anisotropic g factor) the prefactor to the shift due to the dipolar interaction contains $g_{||}^2-g_{\perp}^2$ while the prefactor to the shift due to hyperfine coupling contains $g_{||}^2+2g_{\perp}^2$, where $g_{||}$ and $g_{\perp}$ are respectively the parallel and perpendicular components of the g factor.[19] On the other hand, in the expression for the second moment of the line shape in a system described above the corresponding prefactors are $2g_{||}^2+g_{\perp}^2$ for the dipolar interaction and $g_{||}^2-g_{\perp}^2$ for the hyperfine interaction, respectively.[20] Hence, for a weak g-factor anisotropy the coupling determined from the variation of the shift with susceptibility is dominated by the hyperfine term while that determined from the variation of linewidth with susceptibility is dominated by the dipolar term and/or by macroscopic demagnetization effects. In Ref. 8 we have shown that the hyperfine coupling constant as inferred from the variation of the linewidth with susceptibility is more than 3 times smaller than that determined from the variation of the Knight shift with susceptibility. Furthermore, in the analysis of the linewidth of both ^{7}Li and ^{51}V in Sec. III we have shown that a large part of the broadening is due to macroscopic demagnetization effects. Hence the hyperfine coupling is the dominant coupling producing the Knight shift in LiV_2O_4.

The total measured susceptibility at high T ($\gtrsim$50–100 K) can be written as follows:

$$\chi^{\mathrm{TOT}}(T)=\chi^{\mathrm{VV}}+\chi^{\mathrm{core}}+\chi^{\mathrm{Pauli}}+\chi^{\mathrm{loc}}(T), \tag{2}$$

where χ^{VV} is the orbital Van Vleck susceptibility, χ^{core} is the core diamagnetic susceptibility, χ^{Pauli} is the Pauli paramagnetic susceptibility of conduction electrons, and $\chi^{\mathrm{loc}}(T)$ is the susceptibility of local moments. Since each Li atom is coupled to 4 oxygens, each of which in turn is coupled to 3 vanadium atoms, the ^{7}Li Knight shift can be written as

$$K(T)=K^{\mathrm{VV}}+K^{\mathrm{Pauli}}+K^{\mathrm{loc}}(T)=2\frac{A^{\mathrm{VV}}}{N_A\mu_B}\chi^{\mathrm{VV}}+2\frac{A^{\mathrm{Pauli}}}{N_A\mu_B}\chi^{\mathrm{Pauli}}+12\frac{A^{\mathrm{loc}}}{N_A\mu_B}\chi^{\mathrm{loc}}(T), \tag{3}$$

where the A's are the hyperfine coupling constants and the susceptibilities are expressed in cm^3 per mole of vanadium atoms. The factors of 2 in Eq. (3) account for the two V atoms per formula unit. In the present case the orbital hyperfine coupling A^{VV} is probably negligible for the ^{7}Li nucleus since its valence shell is an orbital singlet. The measured bulk susceptibility in the range 100 to 800 K (Refs. 4, 5, and 21) can be fitted by

$$\chi(T)=\chi_0+\frac{2C}{T-\theta}\equiv\chi_0+\chi^{\mathrm{loc}}(T), \tag{4}$$

with $\chi_0=5.45\times10^{-4}$ cm^3/mol LiV_2O_4, $C=0.329$ cm^3 K/mol V (yielding $g1.873$), and $\theta=-13$ K (see Fig. 1). We thus identify the $\chi^{\mathrm{loc}}(T)$ in Eqs. (2) and (3) with the Curie-Weiss term in Eq. (4). Then by plotting $K(T)$ versus $\chi^{\mathrm{loc}}(T)$ and fitting the data above 100 K to a straight line, as shown in Fig. 3, one obtains from the slope $A^{\mathrm{loc}}=0.18$ (±0.01) kG and from the intercept $K_0=2(A^{\mathrm{Pauli}}/N_A\mu_B)\chi^{\mathrm{Pauli}}=-0.0094\%$. In order to extract the hyperfine constant of the ^{7}Li nuclei with the conduction electrons, A^{Pauli}, one has to estimate the Pauli contribution to the total susceptibility. χ^{VV} has been estimated from a K versus χ analysis[5] of the ^{51}V NMR[7] and bulk susceptibility[5] data on LiV_2O_4 ($\chi^{\mathrm{VV}}=1.19\times10^{-4}$ cm^3/mol V).[5] Using[22] $\chi^{\mathrm{core}}=-31\times10^{-6}$ cm^3/mol V and setting $\chi_0=\chi^{\mathrm{VV}}+\chi^{\mathrm{core}}+\chi^{\mathrm{Pauli}}=2.72\times10^{-4}$ cm^3/mol V we get $\chi^{\mathrm{Pauli}}=1.85\times10^{-4}$ cm^3/mol V, which is about a factor of two larger than that[23] of $LiTi_2O_4$. With this estimate of χ^{Pauli}

we evaluate $A^{\mathrm{Pauli}}=-1.44(\pm 0.02)$ kG. The hyperfine coupling constant A^{Pauli} for Li is only about 1% of the atomic constant for 2*s* electrons[15] as expected for a conduction band predominantly formed by the vanadium *d* electrons. Furthermore, the negative sign indicates that the hyperfine interaction arises from *s* conduction band states below the Fermi energy, which are polarized by antiferromagnetic exchange interaction with the *d* states.

We now analyze the ^{51}V data. Assuming that the Knight shift at the ^{51}V nuclei is dominated by the on-site hyperfine interaction with the electronic V local moment, plus the usual Van Vleck and Pauli terms, we write

$$K(T)=\frac{B^{\mathrm{VV}}}{N_A\mu_B}\chi^{\mathrm{VV}}+\frac{B^{\mathrm{Pauli}}}{N_A\mu_B}\chi^{\mathrm{Pauli}}+\frac{B^{\mathrm{loc}}}{N_A\mu_B}\chi^{\mathrm{loc}}(T), \quad (5)$$

where the *B*'s are the hyperfine coupling constants and the susceptibilities are the same as in Eq. (3). Because the Van Vleck term is not negligible as in the Li case the separate evaluation of the hyperfine constants B^{VV} and B^{Pauli} is not straightforward and will not be attempted here. On the other hand, one can extract with precision B^{loc} in Eq. (5) by fitting a straight line to the plot of *K* versus χ^{loc} (see inset in Fig. 10). From the slope of the linear fit one finds $B^{\mathrm{loc}}=-79$ kG, a value in close agreement with a previous determination[14] (-74 kG) and with the same sign and the same order of magnitude as the nuclear hyperfine constant in vanadium metal[15] ($B^{\mathrm{loc}}=-112$ kG). The intercept of the *K* versus $\chi^{\mathrm{loc}}(T)$ in Fig. 10 yields the *T*-independent portion of Eq. (5). One finds $K_0=0.74\%$. Since B^{Pauli} in Eq. (5) should be dominated by core polarization effects, which yield a negative hyperfine interaction, the positive sign indicates that the positive orbital contribution proportional to χ^{VV} is the dominant one.

2. Spin-lattice relaxation

We discuss the ^{7}Li relaxation data first. In the case of local moments in metals the spin-lattice relaxation of nuclei occurs by two channels. One is the usual Korringa relaxation via conduction electrons and the second is related to magnetic spin fluctuations. The Korringa term estimated on the basis of the *T*-independent K_0 is $1/T_1T=K_0^2/S=5(\pm 1)\times 10^{-3}$ sec^{-1} K^{-1} where $S=(\gamma_e/\gamma_n)^2h/(8\pi^2k_B)$, γ_e and $\gamma_n=2\pi(1655$ Hz/G for ^{7}Li are respectively the electronic and the nuclear gyromagnetic ratios, *h* is Planck's constant, and k_B is the Boltzmann constant. This value may be overestimated since it is a factor of 10 larger than in the isostructural compound $LiTi_2O_4$ (Ref. 16) where there are no local moments. Even taking this upper limit for the Korringa term the contribution to the relaxation rate from this term is still a factor of 10 less than our measured value at room temperature. Hence, spin fluctuations are likely to dominate the nuclear spin-lattice relaxation below room temperature, and in the following we assume the Korringa contribution to be negligible up to 800 K.

The local moment contribution to the spin-lattice relaxation rate is given by[24]

$$\frac{1}{T_1}=\frac{2k_BT\gamma_n^2}{N_A^2g^2\mu_B^2}A^2\Sigma_{\mathbf{q}}(\chi_M''(\mathbf{q},\omega_L)/\omega_L), \quad (6)$$

where *A* is the hyperfine coupling constant, which is assumed to be independent of $\mathbf{q}$, and $\chi_M''(\mathbf{q},\omega_L)$ is the imaginary part of the wave-vector-dependent dynamical susceptibility pertaining to the local moment per mole of magnetic atoms, at the Larmor frequency ω_L. In the limit $\omega_L\rightarrow 0$ the summation is given by $N_A\chi_M^{\mathrm{loc}}(T)\tau/2\pi$ where $\chi_M^{\mathrm{loc}}(T)$ is the static local moment susceptibility per mole and τ is the relaxation time of the electronic spin. In order to estimate the total hyperfine constant *A* in Eq. (6) one has to consider that the ^{7}Li nuclei can be coupled to the V local moments both by a transferred exchange hyperfine interaction and by a direct dipolar interaction. As argued before, the dipolar interaction does not contribute to the measured Knight shift but it would contribute to the relaxation rate. Thus the effective hyperfine interaction squared A^2 is made up of the sum of two terms (we assume that the transferred hyperfine and the dipolar interactions are uncorrelated[17]) $A^2=12(A^{\mathrm{loc}})^2+(A^{\mathrm{dip}})^2$. The first term contains the isotropic transferred hyperfine interaction A^{loc} of a ^{7}Li nucleus with a nearest-neighbor V ion. This quantity is the same as in the Knight shift [see Eq. (3)] and thus one can use the value obtained from the *K* versus χ plot in Fig. 3, i.e., $A^{\mathrm{loc}}=180$ G. The second term is the sum of the square of the transverse local dipolar fields generated at the ^{7}Li nuclear site by the surrounding V local moments. This term was calculated from the known crystal structure[2] by summing over 1000 units cells containing 8 formula units each, and by assuming a complete uncorrelation. For a powder average one has[24] $A^{\mathrm{dip}}=(\sqrt{2\pi}g^2\mu_B^2\Sigma_l r_l^{-6})^{1/2}=2.50$ kG where we used $g=1.873$ from Fig. 1. Thus we obtain $A=\sqrt{12(A^{\mathrm{loc}})^2+(A^{\mathrm{dip}})^2}=2.58$ kG.

Substituting values of various fundamental constants in Eq. (6) we can write

$$\frac{1}{T_1T}=1.73\times 10^{14}\chi_M^{\mathrm{loc}}(T)\tau. \quad (7)$$

It follows that the relaxation rate of the spin of the local moment can be written as

$$\frac{1}{\tau}=1.73\times 10^{14}\chi_M^{\mathrm{loc}}(T)T_1T. \quad (8)$$

By using for $\chi^{\mathrm{loc}}(T)$ the Curie-Weiss term in Eq. (4), we calculate the *T* dependence of $1/\tau$ from our experimental relaxation data ($T>100$ K) as given by Eq. (8). The results are plotted in Fig. 12. We point out that in the traditional heavy-fermion compounds which contain $4f$ local moments and conduction electrons that belong to a different ($3d$) orbital Cox *et al.*[25] have predicted a $T^{0.5}$ dependence for the relaxation rate of the local moment spin. Such a *T* dependence has indeed been experimentally observed in the case of YbCuAl,[25] $CeCu_2Ge_2$,[26] and $YbNi_2B_2C$ (Ref. 27) heavy-fermion compounds. As shown in Fig. 12, a $T^{0.5}$ behavior fits the data reasonably well between 200 and 800 K. If we include lower-*T* data, a better fit to a $T^{0.6}$ power-law behavior is found. It is noted that if the Korringa term is not negligible, as we have assumed, the *T* dependence of $1/\tau$ may be

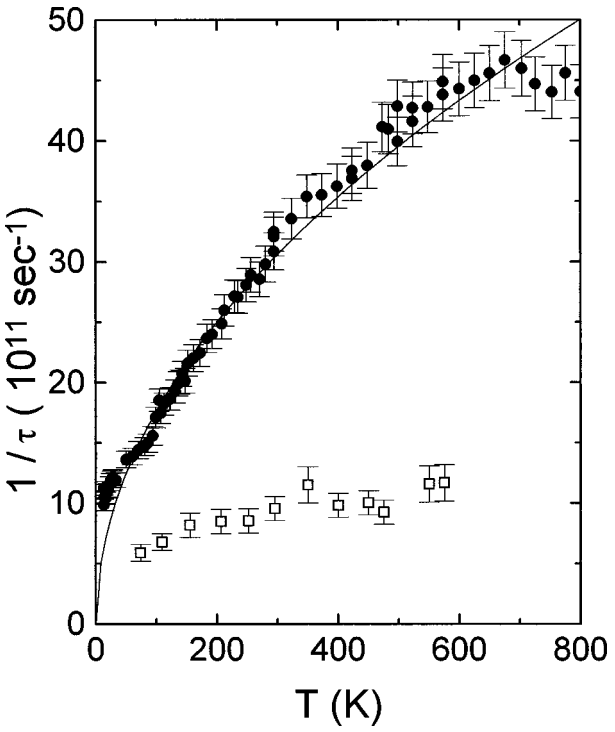

FIG. 12. Vanadium electronic spin-relaxation rate $1/\tau$ vs temperature T, as extracted from ^{7}Li (●) and from ^{51}V (△) nuclear relaxation rates (see text). The solid curve is a $T^{0.5}$ dependence.

found to be different. We remark that in the case of LiV_2O_4, the local moments and the conduction electrons both arise from the three nearly degenerate t_{2g} orbitals. At present, to our knowledge, a theory that can predict the electronic and magnetic properties of such a system does not exist.

The temperature dependence of the local moment relaxation rate $1/\tau$ in Fig. 12 can be analyzed with the following phenomenological model, which should be valid at room temperature and above. We write

$$1/\tau = 1/\tau_d + 1/\tau_{\rm ex}, \tag{9}$$

where the first term corresponds to the spin-lattice relaxation of the impurity spin via conduction electrons and is given by an expression similar to the Korringa law[28]

$$1/\tau_d = (4\pi/\hbar)(k_B T)[J\rho(\epsilon_F)]^2 = \Gamma_0 T, \tag{10}$$

where J is the coupling of the local moments to the band. The second term comes from impurity spin fluctuations due to spin-spin exchange interaction and is given in the limit of high temperatures by[24] $1/\tau_{\rm ex} = \omega_{\rm ex}/2\pi = \Gamma_1$ with $\omega_{\rm ex}^2 = 8J_{\rm ex}^2 zS(S+1)/3\hbar^2$, where $J_{\rm ex}$ is defined such that the Heisenberg exchange term in the Hamiltonian is $2J_{\rm ex}\mathbf{S}_i\cdot\mathbf{S}_j$ where $\mathbf{S}_i$ and $\mathbf{S}_j$ are the nearest-neighbor spins and z is the number of nearest-neighbor spins. For T well above any ordering temperature, $\tau_{\rm ex}$ is expected to be independent of T while τ_d varies inversely with T. Fitting the 300–700 K data to a straight line yields $\Gamma_0 = 4.4(\pm 1)\times 10^9$ sec^{-1} K^{-1} and $\Gamma_1 = 1.9(\pm 0.3)\times 10^{12}$ sec^{-1}, respectively.

From Eq. (10), we now calculate $|J|\rho(\epsilon_F) = 0.05$. Taking the experimentally inferred value of the Pauli susceptibility (above) and using $\chi^{\rm Pauli} = 8N_A\mu_B^2\rho(\epsilon_F)/g^2$ with $g=2$, we find that $\rho(\epsilon_F) = 2.9$ states/(eV vanadium spin direction). This leads to a value of $17(\pm 1)$ meV ($\sim$200 K) for $|J|$, the coupling of the local moments with the conduction electrons. Similarly, from Γ_1 we calculate the exchange coupling $|J_{\rm ex}|$ between the vanadium spins ($S=1/2$ and $z=6$ where z is the number of V nearest neighbors to a given V atom) to be $2.26(\pm 0.03)$ meV ($\sim$ 26 K). This is much smaller than the coupling of the local moment to the band. In a mean-field estimate we can then calculate the corresponding Weiss temperature $|\theta| = 2zS(S+1)|J_{\rm ex}|/3k_B = 78$ K, which is somewhat larger than the Weiss temperature obtained in Fig. 2 from the 100–800 K fit to the susceptibility, i.e., $|\theta| = 13$ K. However, we note that the value of θ obtained by fitting Eq. (4) to $\chi(T)$ data for LiV_2O_4 strongly depends on the temperature range of the fit. For example, Hayakawa *et al.*[21] obtain $\theta \sim -40$ K for the 80–300 K range and $\theta \sim -470$ K for the 600–1000 K range.

Interestingly, in the case of ^{209}Bi NMR in YbBiPt,[29] a heavy-fermion compound, the relaxation rate data at high T have been modeled as coming from local moment fluctuations. However, the authors did not consider the contribution from the exchange coupling between the spins. That this contribution is present is apparent from the nonzero intercept of their $1/\tau$ versus T plot. Extracting the intercept from their plot yields $1/\tau_{\rm ex} = 4\times 10^{12}$ sec^{-1}. We then calculate $|J_{\rm ex}|$ to be 9.5 meV (114 K). This might still be much smaller than the coupling of the local moments to the band. They calculate $|J|\rho(\epsilon_F) = 0.0879$. If one assumes $\rho(\epsilon_F) = 1$ state/eV then $|J| \approx 80$ meV, which is an order of magnitude larger than the coupling between the moments. In the paper by Lysak and MacLaughlin[10] on ^{27}Al NMR in $CeAl_3$, they plot $1/\tau$ versus T on a log-log plot. Their value of $|J_{\rm ex}|$ appears to be about 10 meV. Thus, the local moment–local moment couplings in the rare-earth-based compounds appear to be $\sim$4–5 times that in LiV_2O_4.

We turn now to the ^{51}V relaxation rate data (see Fig. 11). We can extract the relaxation rate of the V local moment $1/\tau$ following the same procedure used for the ^{7}Li T_1 [see Eqs. (6)–(8)]. If we assume that the ^{51}V T_1 is dominated by the hyperfine coupling of the nucleus with the on-site local moment, then we can use for the hyperfine constant A in Eq. (6) the value obtained from the K versus χ plot in the inset in Fig. 10, i.e., $|B^{\rm loc}| = 79$ kG. Thus we find $1/\tau = 7.47\times 10^{16}\chi_M^{\rm loc}(T)T_1T$ assuming $g = 1.873$. By using the Curie-Weiss expression for $\chi_M^{\rm loc}$ in Eq. (4) and the experimental values for the ^{51}V T_1 we obtain the relaxation rate $1/\tau$ shown in Fig. 12. The relaxation rate τ^{-1} of the vanadium local moment derived from the ^{7}Li and ^{51}V spin-lattice relaxation rates should in principle be identical. However, in view of the simplicity of the model and of the fact that we have neglected other contributions (e.g., possible Korringa contributions) to the T_1 for either ^{7}Li and ^{51}V we should consider the agreement in the order of magnitude and in the general temperature behavior of the two sets of values in Fig. 12 as satisfactory.

B. Low-temperature ($\lesssim$20 K) ^{7}Li NMR results

In the above analysis, we have considered the high-T ^{7}Li relaxation data, which can be explained by a V local moment formalism. Around 50 K or so, the ^{7}Li nuclear spin-lattice relaxation rate has a maximum and at low temperatures it

decreases linearly with T as shown in Fig. 6(b). This is precisely the region in T where the shift and the bulk susceptibility have a plateau. In fact, below 100 K the susceptibility in Fig. 1 departs from the fit in terms of a local moment term $\chi^{\rm loc}$ [see Eq. (4)] and the Knight shift is no longer linear in the extrapolated local moment susceptibility $\chi^{\rm loc}$ as it appears in Fig. 3. This then is an indication that at low T the local moments disappear and one is left with a Fermi liquid. Low-T heat capacity data on these samples[4] give a very high coefficient of electronic heat capacity $\gamma(1\ {\rm K})=0.21$ J/(mol V) K^2 (see Ref. 30 for a detailed discussion), indicative of a heavy Fermi liquid. The Korringa ratio K^2T_1T/S is T dependent in the high-T region but becomes constant below about 10 K and has a value of about 0.5 (see Fig. 7 and Table I), close to the value found in normal metals.[15] However, it should be noted that the Korringa ratio of narrow d-band transition metals, with very few exceptions, is significantly larger than unity,[15] which is contrary to the smaller value found here. A possible explanation is related to the presence of local ''impurity'' moments on V defect species. These moments would shorten the measured T_1 without affecting the Knight shift value, thus depressing the Korringa ratio. Although some degree of correlation is seen between the Korringa ratio and the ''impurity'' concentration from inspecting Table I, it can be noted that even for the best samples the Korringa ratio (≈ 0.5) is less than 1.

A constant Korringa product $(T_1T)^{-1}$ has been observed before in other heavy-fermion systems [$YbNi_2B_2C$,[27] $CeAl_3$,[10] $CePd_2In$,[31] and CeCu2Ge$_2$ (Ref. 26)] but an analysis of the Korringa ratio K^2T_1T/S was possible only in $CeAl_3$.[10] It is interesting to note that in this rare-earth heavy-fermion compound a Korringa ratio of the order of two was found at $T<10$ K, which, although greater than unity, is still too low to be consistent with a strongly exchange enhanced Fermi liquid, a situation similar to the one in LiV_2O_4.

V. CONCLUSIONS

In conclusion, we have studied the heavy-fermion compound LiV_2O_4 by ^{7}Li and ^{51}V NMR. Our results demonstrate that LiV_2O_4 exhibits a crossover from local moment behavior at high T ($T\gtrsim 50$ K) to a heavy-Fermi-liquid behavior below about 10 K. In the low-T region the ^{7}Li Knight shift and $1/(T_1T)$ become T independent with a Korringa ratio of about 0.5. In the high-T region ($T\gtrsim 50$ K) the data indicate the existence of local moments. From the T dependence of the ^{7}Li $1/T_1$ we infer an empirical linear T dependence for the local moment relaxation rate above ~ 300 K, and a $T^{0.5}$ dependence if lower-T data are included. This should be compared to the dynamical structure factor determined from future inelastic neutron scattering experiments. Using a simple model, we deduce a coupling of 2.3 meV between the local moments and 17 meV between the local moments and the band. As mentioned earlier, a theory that can model a system that has local moments and conduction electrons that arise out of the same (nearly) degenerate t_{2g} orbitals and that exhibits a crossover to heavy-fermion behavior at low T is called for. Furthermore, we recall that our search for the ^{51}V NMR signal at $T=4.2$ K using pulse techniques was unsuccessful, indicating that the T_1 and/or T_2 are very short ($\leqslant 5\ \mu$sec). One expects that for a normal transition metal T_1 is given by the Korringa ratio $K^2T_1T=pS$ where for ^{51}V $S=3.35\times10^{-6}$ sec K (see Sec. IV A 2) and p is a number that can vary[15] from 1 to 10. For $T=4.2$ K the shortest T_1 is obtained for $p=1$ with $K(4\ {\rm K})=-7.2\%$ (Ref. 7) and is $T_1=1.5\times10^{-4}$ sec; the minimum T_2, due to nuclear-dipolar interaction alone, is of the order of $T_2\simeq 1/\sqrt{\langle\Delta\nu^2\rangle_{\rm dip}}=1/\sqrt{5\times10^7\ {\rm Hz}^2}=1.4\times10^{-4}$ sec [see Eq. (1)]. Thus the T_1 and/or T_2 of ^{51}V at low T ($\leqslant 5\ \mu$sec) must be more than an order of magnitude shorter than what one estimates for a Fermi liquid even allowing for the high density of states at the V sites, i.e., large $|K|$. Thus the question arises about the microscopic nature of the heavy-fermion state in this system. The present findings could be explained if the apparent disappearance of the local moment of the V below $\simeq 30$ K, as seen by the ^{7}Li NMR and magnetic susceptibility, is in fact due to a Kondo-like screening of the V local moment by the conduction electrons. In this case the ^{51}V nucleus would still be strongly coupled to its on-site local moment, presumably giving rise to a very fast relaxation rate. However, the quantitative values of $T_{1,2}$ expected in this case remain to be theoretically elucidated. An additional source of relaxation may be dynamical orbital ordering-correlation-fluctuation effects within the nearly degenerate t_{2g} orbital manifold of each V ion.[32]

ACKNOWLEDGMENTS

Ames Laboratory is operated for the U.S. Department of Energy by Iowa State University under Contract No. W-7405-Eng-82. The work at Ames was supported by the Director for Energy Research, Office of Basic Energy Sciences.

*Permanent address: Department of Physics, Indian Institute of Technology, Powai, Bombay 400 076, India.

† Also at Dipartimento di Fisica Generale ''A. Volta,'' Università di Pavia, 27100, Pavia, Italy.

[1] G. R. Stewart, Rev. Mod. Phys. **56**, 755 (1984).

[2] B. Reuter and J. Jaskowsky, Angew. Chem. **72**, 209 (1960); Ber. Bunsenges. Phys. Chem. **70**, 189 (1966).

[3] D. B. Rogers, J. L. Gillson, and T. E. Gier, Solid State Commun. **10**, 693 (1986).

[4] S. Kondo, D. C. Johnston, C. A. Swenson, F. Borsa, A. V. Mahajan, L. L. Miller, T. Gu, A. I. Goldman, M. B. Maple, D. A. Gajewski, E. J. Freeman, N. R. Dilley, R. P. Dickey, J. Merrin, K. Kojima, G. M. Luke, Y. J. Uemura, O. Chmaissem, and J. D. Jorgensen, Phys. Rev. Lett. **78**, 3729 (1997).

[5] S. Kondo, D. C. Johnston, and L. L. Miller (unpublished).

[6] Y. Ueda, N. Fujiwara , and H. Yasuoka, J. Phys. Soc. Jpn. **66**, 778 (1997).

[7] Y. Amako, T. Naka, M. Onoda, H. Nagasawa, and T. Erata, J. Phys. Soc. Jpn. **59**, 2241 (1990).

[8] D. C. Johnston, T. Ami, F. Borsa, M. K. Crawford, J. A. Fernandez-Baca, K. H. Kim, R. L. Harlow, A. V. Mahajan, L. L. Miller, M. A. Subramanian, D. R. Torgeson, and Z. R. Wang, in *Spectroscopy of Mott Insulators and Correlated Metals*, Springer Series in Solid State Sciences Vol. 119, edited by A. Fujimori and Y. Tokura (Springer-Verlag, Berlin, 1995), pp. 241–254.

[9] The NMR spectrometer employed a new design digital programmable pulse sequencer with a direct digital synthesis (DDS) radio frequency (RF) generator. The system control and acquisition were done by a personal computer using a LabView based program: E. Lee and D.R. Torgeson (unpublished).
[10] M. J. Lysak and D. E. MacLaughlin, Phys. Rev. B **31**, 6963 (1985).
[11] E. Kim and D. L. Cox (unpublished).
[12] O. Chmaissem, J. D. Jorgensen, S. Kondo, and D. C. Johnston, Phys. Rev. Lett. **79**, 4866 (1997).
[13] N. Fujiwara, Y. Ueda, and H. Yasuoka, Physica B **239**, 237 (1997).
[14] M. Onoda, H. Imai, Y. Amako, and H. Nagasawa, Phys. Rev. B **56**, 3760 (1997).
[15] G. C. Carter, L. H. Bennett, and D. J. Kahan, in *Metallic Shifts in NMR*, Progress in Materials Science Vol. 20, edited by B. Chalmers, J. W. Christian, and T. B. Massalski (Pergamon Press, Oxford, 1977).
[16] M. Itoh, Y. Hasegawa, H. Yasuoka, Y. Ueda, and K. Kosuge, Physica C **157**, 65 (1989).
[17] A. Abragam, *Principles of Nuclear Magnetism* (Oxford University Press, New York, 1961).
[18] L. E. Drain, Proc. Phys. Soc. London **80**, 138 (1962).
[19] H. M. McConnell and R. E. Robertson, J. Chem. Phys. **29**, 1361 (1958).
[20] J. A. Ibers, C. H. Holm, and C. R. Adams, Phys. Rev. **121**, 1620 (1961).
[21] T. Hayakawa, D. Shimada, and N. Tsuda, J. Phys. Soc. Jpn. **58**, 2867 (1989).
[22] P. W. Selwood, *Magnetochemistry*, 2nd ed. (Interscience, New York, 1956), p. 78.
[23] D. C. Johnston, J. Low Temp. Phys. **25**, 145 (1976).
[24] T. Moriya, Prog. Theor. Phys. **16**, 23 (1956); J. Phys. Soc. Jpn. **18**, 516 (1963).
[25] D. L. Cox, N. E. Bickers, and J. W. Wilkins, J. Appl. Phys. **57**, 3166 (1985).
[26] N. Buttgen, R. Böhmer, A. Krimmel, and A. Loide, Phys. Rev. B **53**, 5557 (1996).
[27] R. Sala, E. Lee, F. Borsa, and P. C. Canfield, Phys. Rev. B **56**, 6195 (1997).
[28] R. E. Walstedt and A. Narath, Phys. Rev. B **6**, 4118 (1972).
[29] A. P. Reyes, L. P. Le, R. H. Heffner, E. T. Ahrens, Z. Fisk, and P. C. Canfield, Physica B **206-207**, 332 (1995).
[30] D. C. Johnston, C. A. Swenson, and S. Kondo (unpublished).
[31] P. Vonlanthen, J. L. Gavilano, B. Ambrosini, D. Heisenberg, F. Hullinger, and H. R. Ott, Z. Phys. B **102**, 347 (1997).
[32] See, e.g., work on V_2O_3: M. Takigawa, E. T. Ahrens, and Y. Ueda, Phys. Rev. Lett. **76**, 283 (1996); W. Bao, C. Broholm, G. Aeppli, P. Dai, J. M. Honig, and P. Metcalf, *ibid.* **78**, 507 (1997).